Reconstruction of Missing Channel in EEG Using Spatiotemporal Correlation-Based Averaging

Nooshin Bahador, Jarno Jokelainen, Seppo Mustola, Jukka Kortelainen

Objective. Electroencephalogram (EEG) recordings often contain large segments with missing signals due to poor electrode contact or other artifact contamination. Recovering missing values, contaminated segments and lost channels could be highly beneficial, especially for automatic classification algorithms, such as machine/deep learning models, whose performance relies heavily on high-quality data. The current study proposes a new method for recovering missing segments in EEG. Approach. In the proposed method, the reconstructed segment is estimated by substitution of the missing part of the signal with the normalized weighted sum of other channels. The weighting process is based on inter-channel correlation of the non-missing preceding and proceeding temporal windows. The algorithm was designed to be computationally efficient. Experimental data from patients (N = 20) undergoing general anesthesia due to elective surgery were used for the validation of the algorithm. The data were recorded using a portable EEG device with ten channels and a self-adhesive frontal electrode during induction of anesthesia with propofol from waking state until burst suppression level, containing lots of variation in both amplitude and frequency properties. The proposed imputation technique was compared with another simple-structure technique. Distance correlation (DC) was used as a measure of comparison evaluation. Main results.: **The proposed method with average distance correlation of 82.48±10.01 (μ ± σ)% outperformed its competitor with average distance correlation of 67.89±14.12 (μ ± σ)% . This algorithm also showed better performance for an increasing number of missing channels. Significance. the proposed technique provides an easy-to-implement and computationally efficient approach for the reliable reconstruction of missing or contaminated EEG segments.**

***Index Terms*— neural time series, reconstruction, imputation, missing channel, correlation-based averaging, electroencephalography.**

I. Introduction

When it comes to electroencephalography (EEG) recordings as one of the major modalities, widely used for neural systems and rehabilitation applications, there are many sources of variabilities including impedance change, shifts in electrode position, electrode popping and electrode shortcuts [1-3]. These faulty recordings lead to missing channels. Beside faulty electrodes, indigenous sources may also cause contamination, being spatially distributed around their neighboring electrodes. These artifacts with their particular distribution on specific channels create bad data in neighboring channels [4, 5] and may have spectral overlap with neurological activity of interest [6]. Therefore, these contaminated epochs are considered as bad epochs and totally removed from dataset. This may lead to missing large adjacent segments which reduce the amount of useable data and decrease the efficiency of monitoring systems.

Most of the machine learning and deep learning techniques require all channels to be available to the classifier in the decision-making process. If a channel is missing, those methods have no procedure available for exploiting information from remaining non-missing channels. This could lead to wasting potentially complementary information in non-missing channels. It could also happen that in training sets, all channels are available, but in test set, some samples may have one channel missing [7, 8]. To enhance the reliability of monitoring systems and to expand the dataset, estimation of missing values was focus of many researches in recent years. These range from different regression techniques to cluster-based imputation [9-13]. The main problem with these techniques is that their performance is significantly degraded by increasing the missing ratio. Therefore, they cannot be considered as a feasible remedy for the cases in which large adjacent sequences are lost for specific reason, in particular during long-duration artifacts. Furthermore, there has not been an in-depth study on the use of imputation methods for estimating missing channels or missing large segments in neural time series.

So far, there are few studies investigating the reconstruction of missing channel in physiological time series [14-20]. These can be categorized into two major groups of simple and complex techniques. The former group aimed to impute missing channel by taking average of other observed channels. The latter group makes use of machine/deep learning algorithms to impute missing channel based on the most similar features in other observed channels. Although. there is now a growing trend to more sophisticated imputation algorithms, sophisticated approaches may bring more accuracy, they come with other challenges like requirement for a large amount of data and computational resources. In this sense, the methods with simple structure can outperform sophisticated ones. Despite the importance of this issue, there is only a single study in the literature that addressed the imputation problem of missing channels in bio-signals using a simple method [14]. This method is based on weighted summation of other channels

N. Bahador and J. Kortelainen are with physiological Signal Analysis Team, Center for Machine Vision and Signal Analysis, MRC Oulu, University of Oulu, Oulu, Finland.

J. Jokelainen and S. Mustola are with department of Anesthesia, Intensive Care and Pain Medicine at South Carelia Central Hospital, Lappeenranta, Finland.

considering their distance from missing channel. Although the method is simple, it still has some limitations: 1- The technique only focused on location of electrodes. 2- The study explored one scenario including 64 channels in which only a single channel was missed and the performance of method in presence of more missing channels was not investigated.

To this end, this paper aims to develop a simple imputation technique and explore more detailed analysis considering the inter-individual variations as well as the effect of increasing the number of missing channels. The method is based on the concept of statistical dependency structure in multimodal, multivariate and multisensory data with dynamically changing characteristics, the significance of which has been already proven in a wide range of practical applications [21-40].

II. Materials and Methods

A. Data collection and preprocessing

The study was approved by the Northern Ostrobothnia Hospital district local ethics committee (82/2018). Twenty adult patients (table 1) scheduled for an elective surgical operation gave an informed written consent to participate. Patients with cardiovascular or neurological diseases or a body mass index over 30 were excluded. No premedication was used. During the study, the patients were monitored according the standard procedure of the operating room. In addition, EEG was recorded using the BrainStatus self-adhesive electrode and wireless device (Bittium, Oulu, Finland) and a tablet computer on which the signals were observed online. The EEG channels included were Fp1, Fp2, F7, F8, Af7, Af8, Sp1, Sp2, T9, and T10. Reference electrode location was in the middle of forehead. Sampling frequency was 250 Hz. The signals used in the analysis were recorded during the induction of anesthesia with propofol. The procedure included the following steps: 1) Base-line recording of at least 2 min. 2) Beginning of propofol infusion with a fixed rate of 30 mg/kg/h. 3) Observation of the moment for loss of obeying verbal command (LVC) i.e. the time at which the patient stops squeezing anesthesiologist's hand after command ("squeeze my hand"). 4) Observation of the moment for occurrence of burst suppression pattern i.e. the time at which clear suppression periods occur in the EEG. 5) Ending of the recording after at least 2 min of BSP.

The analysis was preceded by high-pass filtering at 0.1 Hz and low-pass filtering at 32 Hz. The 30-second sequences were visually inspected and those sequences including major artifacts were excluded from further analysis.

B. Method

The proposed algorithm for reconstruction of missing channel is based on the weighted summation of signals from observed channels. The weighting process is done considering average temporal-spatial correlation of both preceding and proceeding temporal windows. The correlation is calculated between each channel across all samples within the window. Detailed equations for the proposed method are given in (1) to (3). Figure 1 shows different steps of proposed algorithm. Algorithm 1 presents the steps of reconstructing missing channel using correlation-dependent averaging.

TABLE 1
Patient and data characteristics

Characteristic	Value
Gender (F/M)	12/8
Age, year (Mean±SD)	50.6 ± 15.8
Weight, kg (Mean±SD)	71.9 ± 14.3
Height, cm (Mean±SD)	170.6 ± 9.5
BL* Starting time, min (Mean±SD)	2.9 ± 4.1
Infusion Starting time, min (Mean±SD)	5.5 ± 4.1
LVC* Starting minute, (Mean±SD)	8.9 ± 4.5
BSP* Starting minute, (Mean±SD)	11.5 ± 5.1
SWA* Starting minute, (Mean±SD)	11.3 ± 4.9
SWA Ending minute, (Mean±SD)	12.6 ± 5.0

* BL: baseline, LVC: loss of obeying verbal command, SWA: slow-wave activity, BSP: burst suppression pattern

ALGORITHM I
Algorithm for missing channel reconstruction using correlation-dependent averaging

Input: *len= Window Length, S= Signal, N= Number of windows, j=Missing Channel Index, m=Number of Channels*
Output: $Reconstructed\ Signal$
1: Initialization:
Correlation Matrix of preceding window=[], Correlation Matrix of proceeding window=[] weight=[], $\hat{S}$=[]
2: for n=2 to N-1 do
3: *Correlation Matrix of preceding window=Correlation*$\{S(:,1+len\times(n-1):len\times(n))\}$
4: *Correlation Matrix of proceeding window=Correlation*$\{S(:,1+len\times(n+1):len\times(n+2))\}$
5: *Average Correlation Matrix=*
$$\frac{\{Correlation\ Matrices\ of\ preceding\ window+\ Correlation\ Matrices\ of\ proceeding\ window\}}{2}$$
6: *weight= Average Correlation Matrix(j,*$\{all\ the\ channels-\ jth\ channel\}$*)*
7: $S'=S(\{all\ the\ channels-\ jth\ channel\},1+len\times(n):len\times(n+1))$
8: for k=1:m-1
9: $\hat{S}(k,:)=weight(k)\times S'(k,:)$
10: end for
11: $Reconstructed\ Signal=\ summation(\hat{S},1)/summation(weight)$
12: end for
13: return $Reconstructed\ Signal$

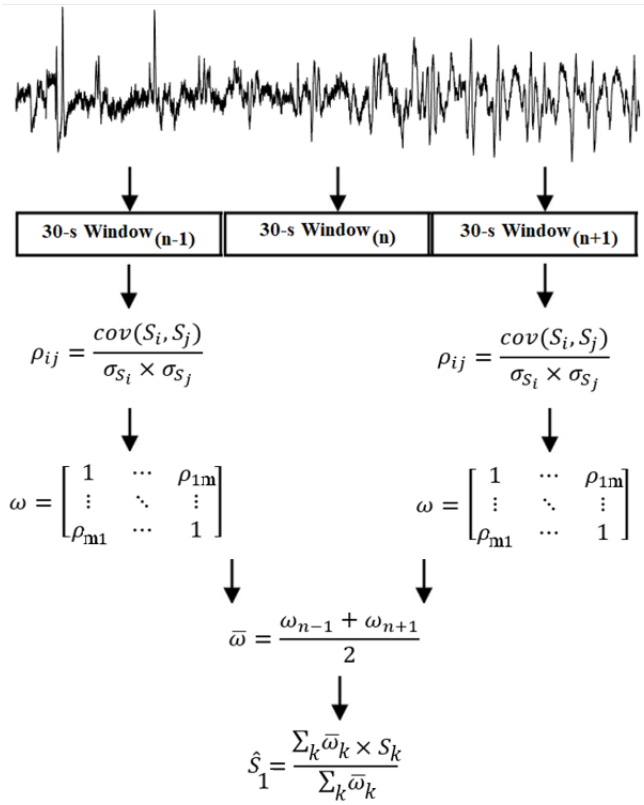

Fig. 1. Proposed algorithm for recovering missing channel of number one (S_1); Employing weighted average of the signals from other channels (S_2, …, S_m) associated with the n^{th} window. The weighting is done considering average spatial correlation of $(n-1)^{th}$ and $(n+1)^{th}$ windows

Weight matrix can be formed based on pairwise correlation coefficient of channels according to (1).

$$\omega = \begin{bmatrix} \rho_{11} & \rho_{12} & \rho_{13} & \cdots & \rho_{1(m-1)} & \rho_{1m} \\ \vdots & \vdots & \vdots & \vdots & \vdots & \vdots \\ \rho_{m1} & \rho_{m2} & \rho_{m3} & \cdots & \rho_{m(m-1)} & \rho_{mm} \end{bmatrix} \tag{1}$$

which m is total number of channels,

and $\rho_{ij} = \frac{cov(S_i, S_j)}{\sigma_{S_i} \times \sigma_{S_j}}$.

S_i and S_j are respectively signals of i^{th} and j^{th} channels.

By taking average and normalizing weight matrices of preceding and proceeding windows according to equations of (2) and (3), the synthetic version of signal is reconstructed.

$$\bar{\omega} = \frac{\omega_{n-1} + \omega_{n+1}}{2} = 0.5 \times \begin{bmatrix} {\rho_{11}}^{n-1} + {\rho_{11}}^{n+1} & \cdots & {\rho_{1m}}^{n-1} + {\rho_{1m}}^{n+1} \\ \vdots & \ddots & \vdots \\ {\rho_{m1}}^{n-1} + {\rho_{m1}}^{n+1} & \cdots & {\rho_{mm}}^{n-1} + {\rho_{mm}}^{n+1} \end{bmatrix} \tag{2}$$

$$\hat{S}_1 = \frac{\sum_k \bar{\omega}_k \times S_k}{\sum_k \bar{\omega}_k} = \frac{(\bar{\omega}_2 \times S_2) + \cdots + (\bar{\omega}_m \times S_m)}{\bar{\omega}_2 + \cdots + \bar{\omega}_m} \tag{3}$$

The matrix $\bar{\omega}$ includes k rows and k columns which correspond to the k channels. This matrix is a symmetric matrix, therefore only first row of this matrix is considered, and each element within this row is multiplied by its corresponding channel.

The proposed weighting was inspired by general expression used for weighted average formula in the literature [13, 14, 18, 41-43].

C. Comparison to a Previous Method

A commonly used approach for reconstructing a missing EEG channel is weighted averaged of neighboring electrodes. The weighting process in this method is performed based on Euclidian distance of neighboring channels from the one which is missing. The hypothesis in this technique is that closer electrodes provides more information regarding the variations in missing channel in compared to those which are farther away. The mathematical expression for this method is expressed as follow [14]:

$$\hat{S} = \frac{\sum_{i \neq j} w_{ij} \times S_j}{\sum_{i \neq j} w_{ij}} \tag{4}$$

$$w_{ij} = \frac{1}{L_{ij}}$$

$$L_{ij} = \sqrt{(x_i - x_j)^2 + (y_i - y_j)^2 + (z_i - z_j)^2}$$

where w_{ij} refers to the inverse Euclidean distance between two electrode positions of i and j, being calculated from the cartesian coordinate of each electrode position.

$i \neq j$ means that only off-diagonal elements of distance matrix are used which represent distance between pairs of channels.

Algorithm 2 presents the steps of reconstructing missing channel using weighted averaged of neighboring electrodes.

A comparison study was conducted to evaluate the performance of this method and compare it with proposed algorithm. This comparison study was performed under different scenarios of increasing number of missing channels. The metric used for performance evaluation was distance correlation. The within-subject and between-subject variability of these distance correlations was also characterized as a function of the number of missing channels.

D. Performance metric

Distance correlation (DC), being used as performance metric in this study, measures both linear and nonlinear association between two signals and can be computed according to the following steps.

1- Computing Euclidean distance (Ed) for all pairwise distances:

$$Ed_{ij} = Ed(x_i, x_j) = \sqrt{\sum_{k=1}^{n} (x_{ik} - x_{jk})^2} \tag{5}$$

2- Taking double centered distance:

$$\overline{Ed}_{ij}(\cdot) = Ed_{ij}(\cdot) - \overline{Ed}_{i\cdot}(\cdot) - \overline{Ed}_{\cdot j}(\cdot) + \overline{Ed}_{\cdot\cdot}(\cdot) \tag{6}$$

3- Computing arithmetic average of products of S_1 and S_2 as follow:

$$dCov(S_1, S_2) = \frac{1}{n^2} \sum_{ij} \overline{Ed}_{ij}(S_1) \cdot \overline{Ed}_{ij}(S_2) \tag{7}$$

4- Computing distance variances:

$$dVar(S_1) = \frac{1}{n^2} \sum_{ij} \overline{Ed}_{ij}(S_1)^2 \tag{8}$$

$$dVar(S_2) = \frac{1}{n^2} \sum_{ij} \overline{Ed}_{ij}(S_2)^2$$

5- Computing distance correlation:

$$dCor(S_1, S_2) = \frac{dCov(S_1, S_2)}{\sqrt{dVar(S_1) \cdot dVar(S_2)}} \tag{9}$$

III. Result

A. Results of implementing method

The average and standard deviation values of distance correlation was calculated per subject, and then the distribution of these values across all subjects was computed based on average, median, minimum and maximum values (Table 2).

For illustration, figure 2 shows the original signal of one EEG channel and its recovered version based on proposed technique. The computed corresponding distance correlation for this example was 95.14 %, suggesting a strong statistical relationship between original and recovered signals.

TABLE 2
Distribution of distance correlation across all subjects

Parameters	Proposed Method		Euclidean distance-based method	
	Mean	Std	Mean	Std
Mean	82.48	10.01	67.89	14.12
Median	84.07	10.09	71.47	13.02
Maximum	92.87	21.0	80.78	23.37
Minimum	40.02	3.3	31.57	6.96

Comparing the visual inspection of spectrogram plots for both original signal and its recovered version indicates a good performance of the proposed reconstruction method in recovering temporal-spectral progression patterns within the original EEG signal.

The distribution of the amplitude and its variability in both original signal and its recovered version are respectively given in figure 4 and 5. According to these figures, the recovered signal follows almost the same distribution as original one. It should be noted that uniform amplitude scaling seen in the results has no effect on the correlation measures [44]. However, using normalization, the uniform amplitude scaling can be eliminated.

ALGORITHM 2
Algorithm for missing channel reconstruction using weighted averaged of neighboring electrodes

Input: *len= Window Length, S= Signal, N=Number of windows, j=Missing Channel Index, m=Number of Channels*
Output: $Reconstructed\ Signal$
1: Initialization:
XY=Electrode positions
Distance Matrix = Computes a matrix of pair-wise distances between XY points using Euclidean method
weight=[], $\hat{S}$*=[]*
2: for n=1 to N do
3: weight= Distance Matrix
4: $S' = S(\{all\ the\ channels - jth\ channel\}, 1 + len \times (n): len \times (n+1))$
5: for k=1:m-1
6: $\hat{S}(k,:) = weight(k) \times S'(k,:)$
7: end for
8: $Reconstructed\ Signal = summation(\hat{S}, 1)/summation(weight)$
9: end for
10: return $Reconstructed\ Signal$

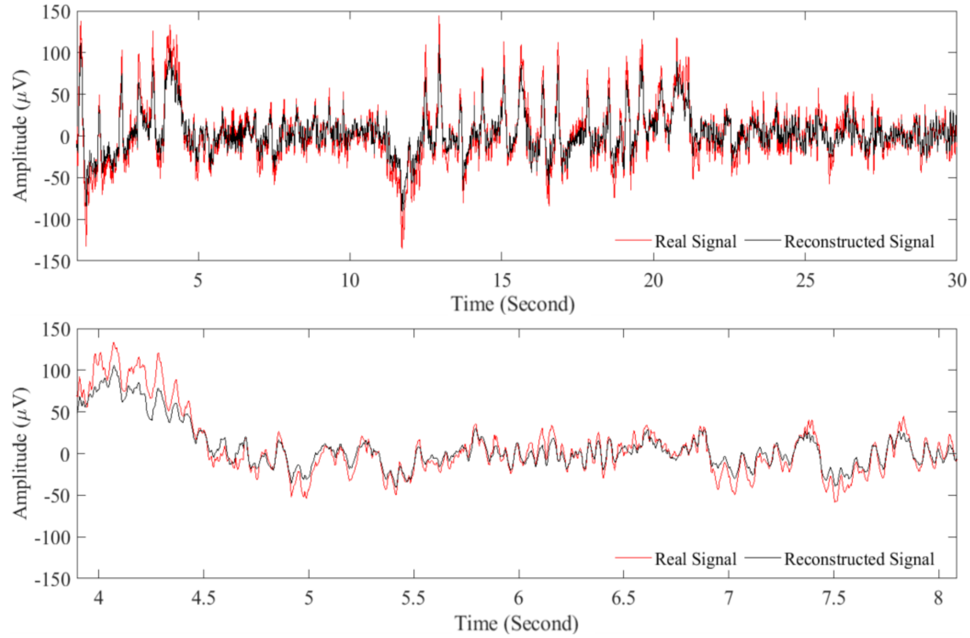

Fig. 2. Comparison between original signal of one EEG channel with its recovered version for distance correlation of 95.14 % (Second plot is enlarged version of first plot)

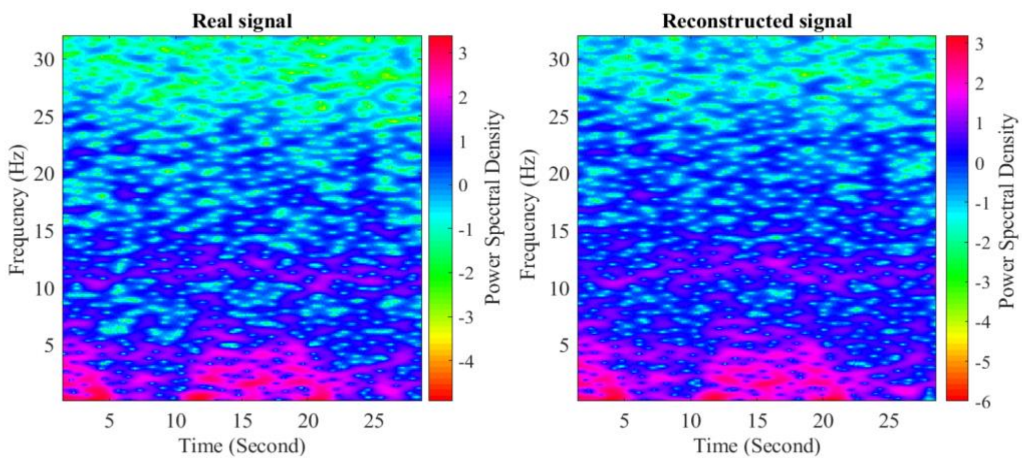

Fig. 3. Temporal-spectral progression patterns within original signal of one EEG channel and its recovered version for distance correlation of 95.14 %

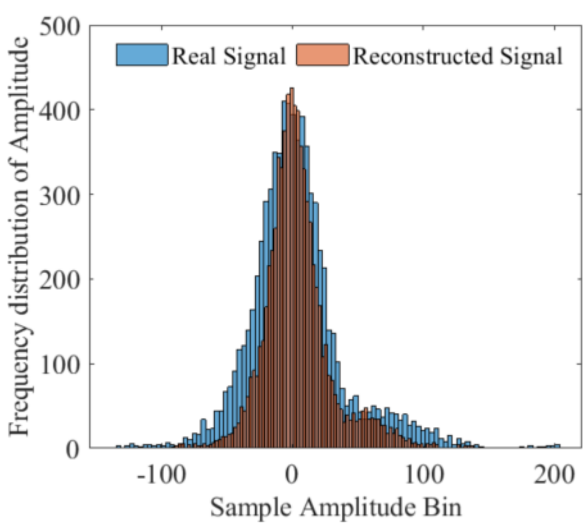

Fig. 4. Distribution of original signal and its recovered version for distance correlation of 95.14 %

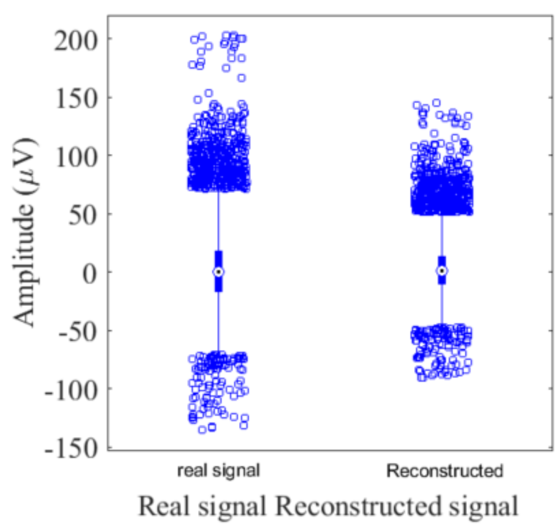

Fig. 5. Variability within original signal and its recovered version for distance correlation of 95.14 %

B. Results of increasing number of missing channels

To further analyze the effectiveness of proposed method, different scenarios of increasing number of missing channels were implemented. The electrodes being removed in each scenario according to table 3 (Scenario 1-5).

According to the figures of 6 to 9, although the degradation rate of reconstruction accuracy increases with growing number of missing channels, the recovered version of signal still follows the temporal-spectral progression patterns within the original EEG signal.

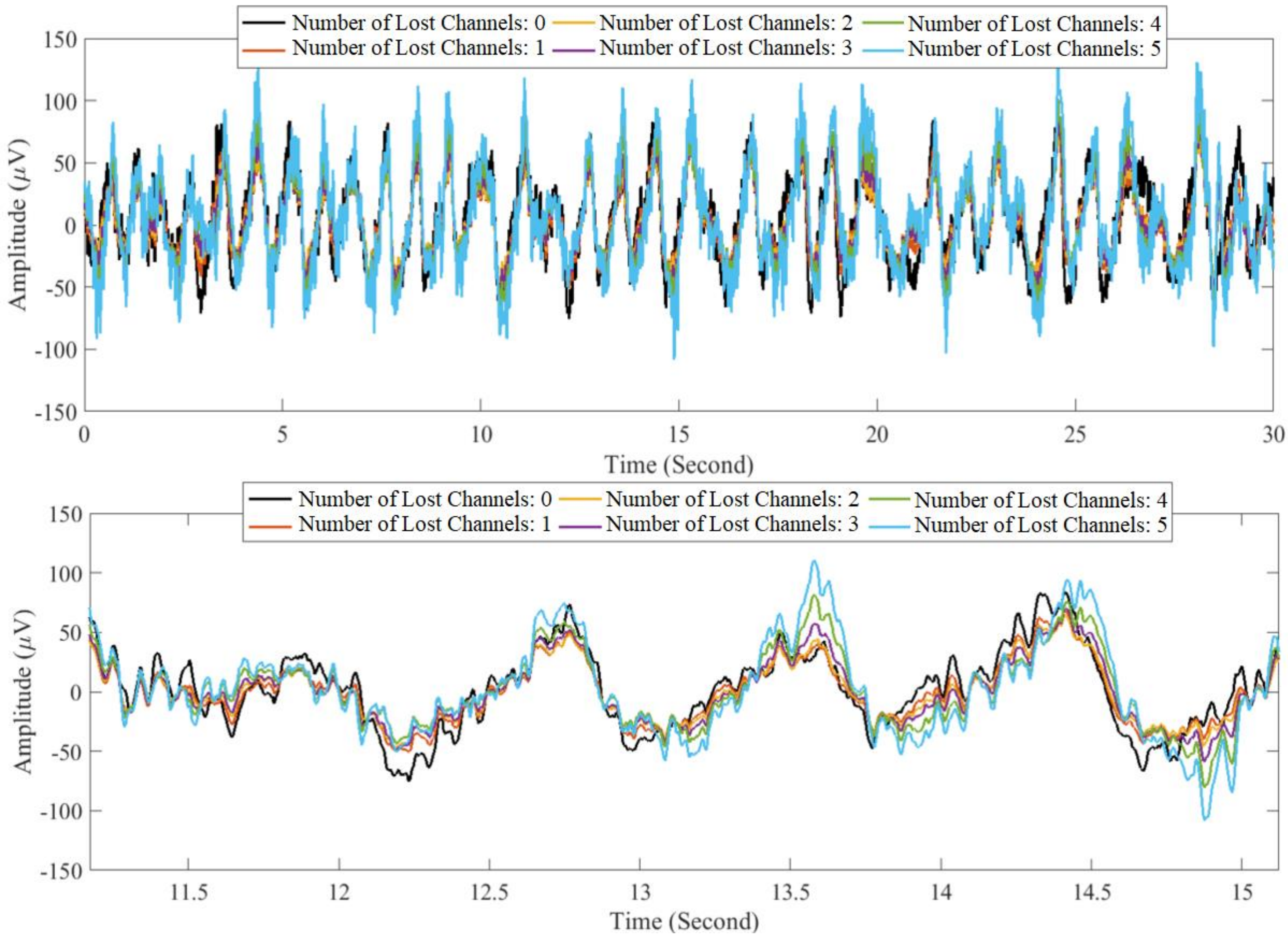

Fig. 6. Changes in temporal patterns of recovered signal with increasing number of lost channels (Second plot is enlarged version of first plot)

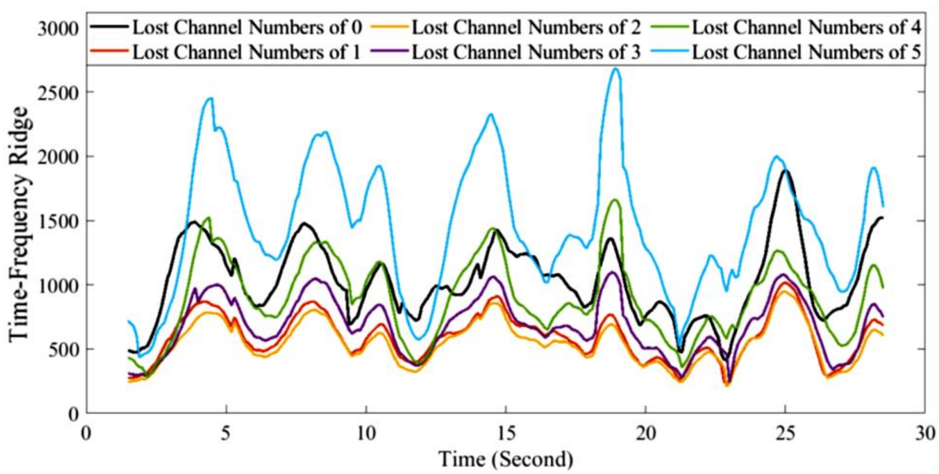

Fig. 7. Changes in temporal-spectral progression patterns of recovered signal with increasing number of lost channels

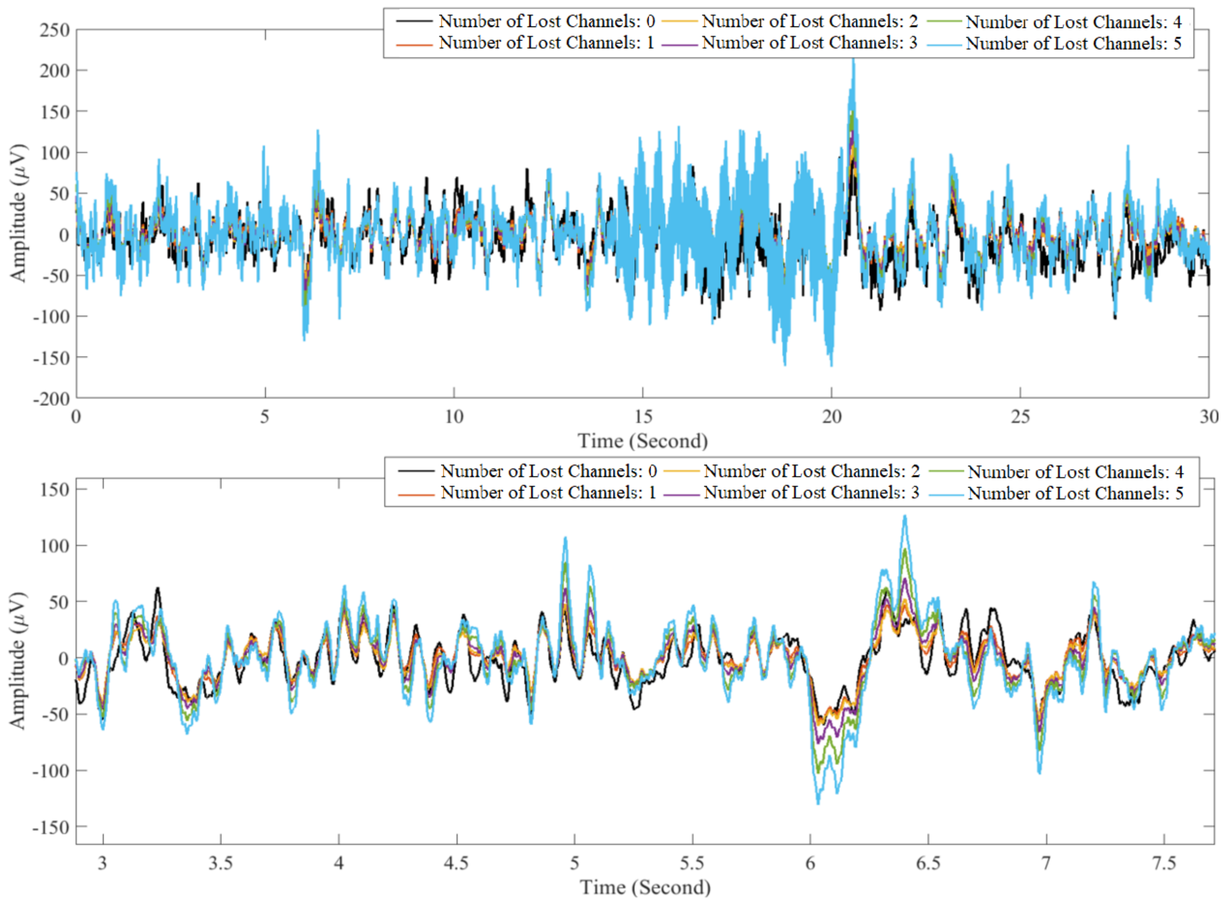

Fig. 8. Changes in temporal patterns of recovered signal with increasing number of lost channels (Second plot is enlarged version of first plot)

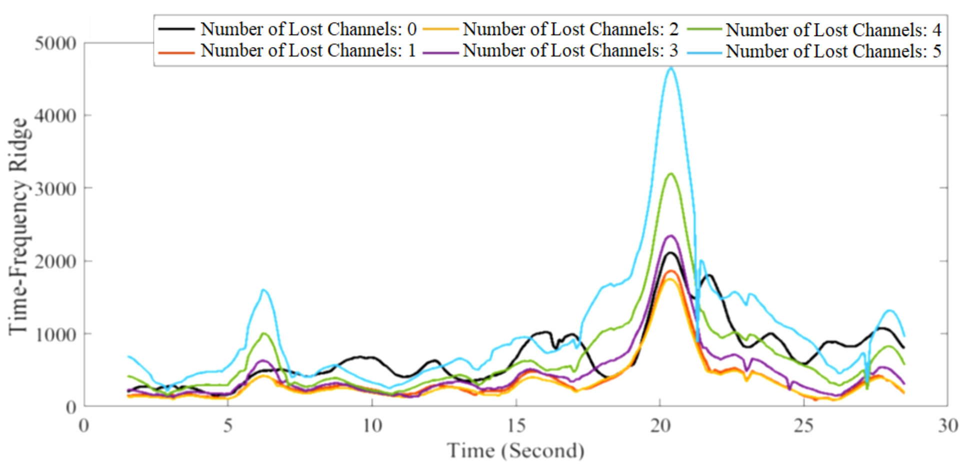

Fig. 9. Changes in temporal-spectral progression patterns of recovered signal with increasing number of lost channels

C. Inter-subject and intra-subject variation

Chart 10 shows inter-subject and intra-subject variation of average correlation coefficient across all channels. Chart 11 illustrates the inter-subject variation in distance correlation of reconstructed channel.

D. Statistical analysis of within subject variability

The performance of proposed technique was evaluated and compared with that of presented in [11]. The electrodes being removed in each scenario are given in table 3. According to the statistical analysis of within subject variability (Table 4 and Figures of 12), there was a difference between the Coefficient of Variability of DC obtained by proposed method and Coefficient of Variability of DC obtained by Euclidean distance-based method. A t-test showed this difference was statistically significant, $t(7) = -5.1$, $p = 0.001$, 95% confidence interval (-10.98, -4.02). The within subject variability of distance correlation for proposed method had lower values (M = 19.65, SD = 4.5) than the within subject variability of distance correlation for Euclidean distance-based method (M = 27.15, SD = 5.9).

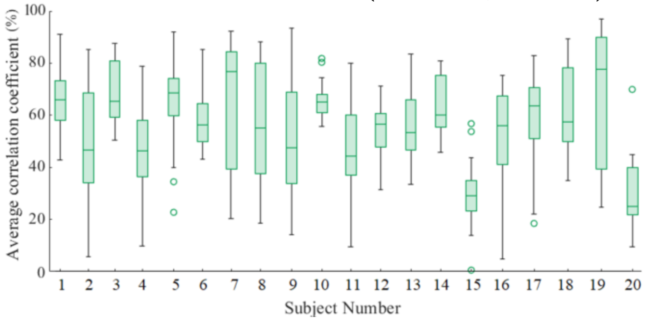

Fig. 10. Inter-subject and Intra-subject variation of average correlation coefficient between channels of each temporal window

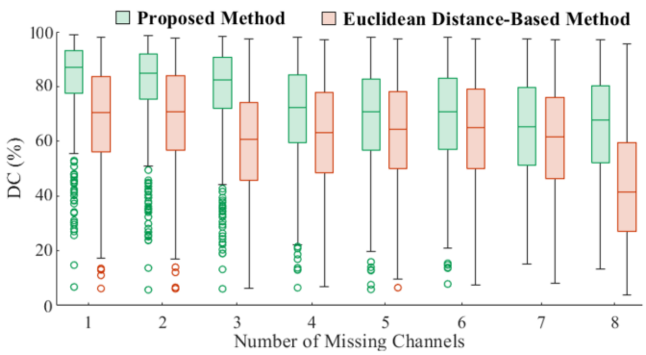

Fig. 11. Inter-subject variation in DC obtained for different numbers of missing channel

TABLE 3
Lost channels in each scenario

1	2	3	4	5	6	7	8
'T10'	'T10' 'Af8'	'T10' 'Af8' 'F8'	'T10' 'Af8' 'F8' 'Fp2'	'T10' 'Af8' 'F8' 'Fp2' 'Fp1'	'T10' 'Af8' 'F8' 'Fp2' 'Fp1' 'T9'	'T10' 'Af8' 'F8' 'Fp2' 'Fp1' 'T9' 'F7'	'T10' 'Af8' 'F8' 'Fp2' 'Fp1' 'T9' 'F7' 'Sp1'

E. *Statistical analysis of between subject variability*

According to the statistical analysis of between subject variability (Table 4 and Figures of 13), there was a difference between Coefficient of Variability of DC obtained by proposed method and Coefficient of Variability of DC obtained by Euclidean distance-based method (Considering distance correlation as performance metric). A t-test showed this difference was statistically significant, $t(7) = -5.58$, $p = 0.001$, 95% confidence interval (-5.42, -2.19). The between subject variability of distance correlation for proposed method had lower values (M = 16.32, SD = 1.51) than the between subject variability of distance correlation for Euclidean distance-based method (M = 20.12, SD = 1.86).

TABLE 4
Statistical analysis

Statistics

		Mean			Std. Deviation			Std. Error Mean		
	N	within subject CV data	between subject CV data	Overall DC data	within subject CV data	between subject CV data	Overall DC data	within subject CV data	between subject CV data	Overall DC data
Proposed method	8	19.65	16.32	71.87	4.5	1.51	7.08	1.59	0.53	2.5
Euclidean distance-based method	8	27.15	20.12	60.84	5.9	1.86	7.71	2.09	0.66	2.73

t-Test for paired samples

	t			df			p-value (2-tailed)		
	within subject CV data	between subject CV data	Overall DC data	within subject CV data	between subject CV data	Overall DC data	within subject CV data	between subject CV data	Overall DC data
Proposed method - Euclidean distance-based method	-5.1	-5.58	4.59	7	7	7	0.001	0.001	0.003

95% Confidence interval of the difference

	Mean			Std. Deviation			Std. Error Mean			Lower			Upper		
	within subject CV data	between subject CV data	Overall DC data	within subject CV data	between subject CV data	Overall DC data	within subject CV data	between subject CV data	Overall DC data	within subject CV data	between subject CV data	Overall DC data	within subject CV data	between subject CV data	Overall DC data
Proposed method-Euclidean distance-based method	-7.5	-3.8	11.03	4.16	1.93	6.8	1.47	0.68	2.4	-10.98	-5.42	5.35	-4.02	-2.19	16.71

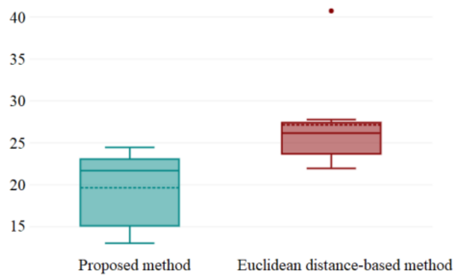

Fig. 12. Distribution of within subject variability of Coefficient of Variability

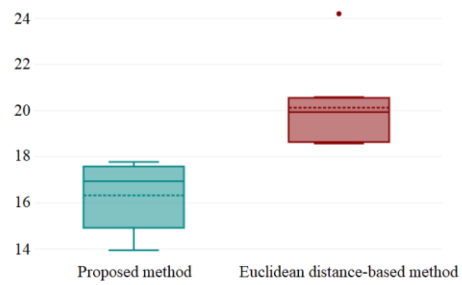

Fig. 13. Distribution of between subject variability of Coefficient of Variability

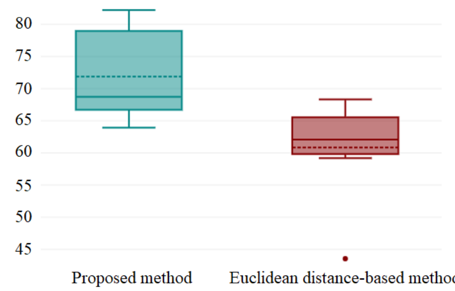

Fig. 14. Distribution of distance correlation

F. *Statistical analysis of performance*

According to the statistical analysis of performance (Table 4 and Figures of 14), there was a difference between the DC obtained by proposed method and DC obtained by Euclidean distance-based method (Considering distance correlation as performance metric). A t-test showed this difference was statistically significant, $t(7) = 4.59$, $p = 0.003$, 95% confidence interval [5.35, 16.71]. The distance correlation for proposed method had higher values ($M = 71.87$, $SD = 7.08$) than the distance correlation for Euclidean distance-based method ($M = 60.84$, $SD = 7.71$).

G. *Investigating the effect of window length on the results*

According to figure 15, difference between average distance correlation obtained from proposed method and average distance correlation obtained from Euclidean distance-based method is higher for windows with shorter length. In general, the difference is significant for different window lengths.

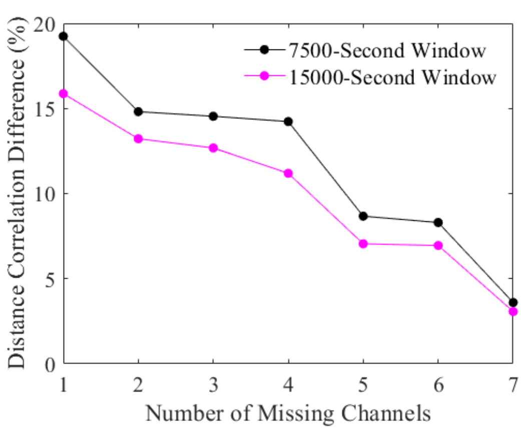

Fig. 15. Difference between average distance correlation obtained by proposed method from DC obtained by Ed method for different window lengths and different numbers of missing channel (difference between two DC values in %-units)

IV. Discussion

There are a limited number of studies exploring the imputation of missing channel in physiological signals, being categorized into two major groups of simple and complex techniques according to Table 5. Although the simplest approaches can outperform the more sophisticated ones in practical applications due to their fast speed, easy implementation and lower memory requirement, there is only one study in the literature, focusing on simple channel reconstruction in physiological signals [14]. This study imputed one missing channel based on a weighted average of observed channels, placing greater weight for spatially closer EEG channels. Despite the straightforward structure of this method, its performance degradation by increasing the number of missing channels was not investigated. Furthermore, this study has not taken into account subject-dependency of bio-signals. These signals can be highly subjective, and the performance of algorithm can change with different study subjects.

Considering the issue with earlier approach, current paper aimed to develop a simple correlation-based averaging approach for missing data imputation and provided an in-depth analysis by considering the inter-individual variations in bio-signal patterns as well as the effect of increasing the number of missing channels. The idea behind proposed reconstruction method was taking statistical dependency of multisensory data into consideration. This statistical dependency including spatio-temporal correlation patterns is captured through moving window and then integrated by local averaging to reconstruct missing EEG channel. The importance of considering statistical dependencies has been already proven in a wide range of practical applications summarized in table 6 [21-40]. Most of these techniques focused on reconstructing data based on correlation between patterns, correlation between envelopes and similarity between shapes and trajectories of data [24-29]. Some also emphasized on local correlation and similarity between neighboring sensors [38-39]. Furthermore, the EEG signals are result of brain activity and different channels monitor the same activity from different locations. Since, the source for all the signals is the same, it is likely that the EEG signals from different channels are correlated. Different cortical locations have also different degrees of correlation [15-17]. Therefore, considering the important role of correlation concept in neural signal reconstruction, this study tried to create a decaying weighting function which place more emphasis on highly correlated channels than those that are less correlated. Moreover, since the proposed method is not based on electrodes position, it does not need to adopt for different set of electrodes and different scalp maps as every single subject has unique geometry and shape of the head [14].

The major contributions in this study are summarized as follows: 1- The proposed reconstruction technique considered heterogonous nature of physiological time series due to the variability in time-frequency characteristic over long-duration monitoring by embedding information within both preceding and proceeding temporal windows. 2- The proposed method embedded inter-channel dependency of neural time series by considering temporal-spatial correlation. 3- The current study investigated the performance degradation of reconstruction with increase in the number of missing channels. 4- The current study explored the performance of imputation for inter-individual variability by analyzing different subjects. 4- Reconstruction of missing channels was performed on a dataset captured by 10-channel forehead self-adhesive electrodes. 5- Reconstruction technique performance was evaluated on dataset associated with measurements during different stages of anesthesia induction in which the EEG time-frequency characteristic varies a lot.

Considering the results of current study, distance correlation of reconstructed signals using proposed algorithm was 21.5% higher, on average, than those of being reconstructed by the earlier approach (82.5% vs. 67.7%, see Table 2). The proposed technique also showed more robustness for loosing several channels. This easy-to-implement approach would be computationally efficient due to its simple structure. It also requires no learning process and hyperparameter optimization. The limitation of this technique is that it could be only applicable for multichannel recordings.

TABLE 5
Literature review of reconstruction techniques for missing channel in physiological time series

Type of Method		**Details**	**Modality**
Simple Approaches		Normalized weighted summation of other channels considering inverse distance [14]	EEG
Complex Approaches	Methods Based on Optimization	Row-sparse recovery by exploiting the transform domain sparsity considering inter-channel correlation in which sparse transform domain coefficients are reconstructed by solving an optimization problem [15, 16]	EEG
		Applying Karhunen Loeve transform and solving an optimization problem with sparsity constraint to learn the inter-channel correlation, and then using learnt correlation to reconstruct missing channel [45]	EEG
	Methods Based on Deep Learning	Recovering missing channel by feeding raw signals of other channels to a Long Short-Term Memory (LSTM) Recurrent Neural Network (RNN) [17]	EEG
		Mapping channels into a tensor that reflects the special locations of electrode and then feeding it into a deep encoder-decoder network [18]	EEG
		Recovering missing channel by feeding other channels into a deep neural network [19]	EMG
		Predicting missing channel by feeding other channels into a focused time-delayed neural network, distributed time-delayed neural network, and nonlinear autoregressive network [20]	ECG

TABLE 6
Literature review of reconstruction techniques considering statistical dependencies

Method	Details	Application
✓ Hierarchical correlation reconstruction [21]	Local averaging over past values considering probability distribution and applying exponentially decaying weights	Non-stationary time series
✓ Spearman's rank correlation coefficient [22]	Monotonically quantifying correlation between two time-series in high-dimensional data	High dimensional chemical data
✓ Pairwise ✓ correlations [23]	Considering n-dimensional joint probability distribution	Biological data
✓ Cross-modal interaction [24]	Correlation coefficient between envelopes	Speech signals
✓ Correlation patterns [25]	Correlation patterns as a function of time	Climatic signal
✓ Correlation caused by ✓ the underlying trend in the time-series [26]	Based on Pearson correlation coefficient Based on producing moment correlation coefficient	Climatic time-series
✓ Correlations between different modalities [27]	Inter-series correlation based on average Pearson correlation coefficient	Temperature signal
✓ Locally adaptive linear interpolation [28]	Maintaining the essential shape of the time-series trajectory	Remote sensing time series data
✓ Global correlation information [29]	Based on Pearson correlation coefficient	Synthetic Time Series

✓	Spatio-temporal correlation patterns [30]	Based on Pearson correlation coefficient and search neighborhood	Hydrological flow rate time-series
✓	Spatiotemporal context dependencies [31]	Based on linear state transition matrix	Network traffic traces
✓	Spatiotemporal covariance in order to take both temporal and spatial correlations [32]	Based on decomposing a spatiotemporal covariance into different modes and then selects the optimal set of modes for reconstruction	Remote sensing data
✓	Temporal covariance [33]	Based on solving the eigenvalue problem, and choosing an optimal number of empirical orthogonal functions for reconstruction	Remote sensing data
✓	Similarity between two temporal patterns [34]	Using binary space partitioning trees	Time series of multispectral images
✓	Joint probability distribution over the variables [35]	Considering the mean and covariance matrix	Industrial time series
✓	Spatial-temporal correlation [36]	Based on low-rank matrix factorization	Traffic network data
✓	Phase Space Reconstruction based on extracting linear correlation between sequences [37]	Using autocorrelation function method for finding the delay time	Vegetation Temperature Condition Index time series data
✓	Correlation between different neighboring sensors [38]	Using linear regression models on spatially correlated measurements	Distribution water network flowmeters data
✓	Spatial-spectral-temporal strategy [39]	Using a local patch-based similarity	Satellite image time series
✓	Spatio-temporal correlation [40]	Considering binary regression	Time traffic flow data

V. Conclusion

This study presented a simple method for implementing missing channel imputation on neural time series based on temporal-spatial correlation. The result showed that the proposed algorithm outperforms the Euclidean distance-based weighted reconstruction [14]. This method has the benefit of simple structure and no requirement for any training or hyper parameter tuning. Considering only preceding windows, this algorithm with its low computational complexity can be also adapted for real-time reconstruction. The proposed method has also potential to use in data augmentation and generating synthetic time series from the existing ones which could be highly beneficial in enhancing machine/deep learning algorithms. Regarding these, a further investigation will be conducted in future.

VI. ACKNOWLEDGMENT

This work was supported by Grant no. 308935 from the Academy of Finland and Infotech. Nooshin Bahador would also like to thank Orion Research Foundation sr, Walter Ahlström Foundations and Tauno Tönningin Säätiö for their support.

REFERENCES

[1] Bahador N, Jokelainen J, Mustola S and Kortelainen J 2021 Multimodal spatio-temporal-spectral fusion for deep learning applications in physiological time series processing: a case study in monitoring the depth of anesthesia Inform. Fusion 73 125–43 ISSN 1566-2535

[2] Bahador N, Ferreira D, Tamminen S and Kortelainen J 2021 Deep learning-based multimodal data fusion: case study in food intake episodes detection using wearable sensors JMIR mHealth uHealth 9 e21926

[3] Bahador N, Erikson K, Laurila J, Koskenkari J, Ala-Kokko T and Kortelainen J 2020 A correlation-driven mapping for deep learning application in detecting artifacts within the EEG J. Neural. Eng. 17 056018

[4] Bahador N, Erikson K, Laurila J, Koskenkari J, Ala-Kokko T and Kortelainen J 2020 Automatic detection of artifacts in EEG by combining deep learning and histogram contour processing 2020 42nd Annual Int. Conf. of the IEEE Engineering in Medicine & Biology Society (EMBC) pp 138–41

[5] Bahador N, Zhao G, Jokelainen J, Mustola S and Kortelainen J 2021 Morphology-preserving reconstruction of times series with missing data for enhancing deep learning-based classification Biomed. Signal Process. Control. 70 103052 ISSN 1746-8094

[6] Daly I, Scherer R, Billinger M and Müller-Putz G 2015 FORCe: fully online and automated artifact removal for brain-computer interfacing IEEE Trans. Neural. Syst. Rehabil. Eng. 23 725–36

[7] Sharma A and Hamarneh G 2020 Missing MRI pulse sequence synthesis using multi-modal generative adversarial network IEEE Trans. Med. Imaging 39 1170–83

[8] Poh N, Windridge D, Mottl V, Tatarchuk A and Eliseyev A 2010 Addressing missing values in kernel-based multimodal biometric fusion using neutral point substitution IEEE Trans. Inform. Forensics Secur. 5 461–9

[9] Mostafa S M 2019 Imputing missing values using cumulative linear regression CAAI Trans. Intell. Technol. 4 182–200

[10] Razavi-Far R, Farajzadeh-Zanjani M, Saif M and Chakrabarti S 2020 Correlation clustering imputation for diagnosing attacks and faults with missing power grid data IEEE Trans. Smart Grid 11 1453–64

[11] Nair S S, French R M, Laroche D and Thomas E 2010 The application of machine learning algorithms to the analysis of electromyographic patterns from arthritic patients IEEE Trans. Neural. Syst. Rehabil. Eng. 18 174–84

[12] Lai X, Zhang L and Liu X 2020 Takagi-sugeno modeling of incomplete data for missing value imputation with the use of alternate learning IEEE Access 8 83633–44

[13] Wang P and Chen X 2020 Three-way ensemble clustering for incomplete data IEEE Access 8 91855–64

[14] Courellis H S, Iversen J R, Poizner H and Cauwenberghs G 2016 EEG channel interpolation using ellipsoid geodesic length

2016 IEEE Biomedical Circuits and Systems Conf. (Biocas) (Shanghai) pp 540–3
[15] Shukla A and Majumdar A 2015 Exploiting inter-channel correlation in EEG signal reconstruction Biomed. Signal Process. Control. 18 49–55
[16] Aghababaei M H and Azemi G 2020 A modified row-sparse multiple measurement vector recovery algorithm for reconstructing multichannel EEG signals from compressive measurements Biomed. Signal Process. Control. 60 101956
[17] Paul A 2020 Prediction of missing EEG channel waveform using LSTM 2020 4th Int. Conf. on Computational Intelligence and Networks (CINE) (Kolkata, India) pp 1–6
[18] Saba-Sadiya S, Alhanai T, Liu T and Ghassemi M M 2020 EEG channel interpolation using deep encoder-decoder networks (arXiv:2009.12244)
[19] Wang P, Tan E, Jin Y, Li L and Wang J 2018 Prediction of EMG signal on missing channel from signal captured from other related channels via deep neural network 2018 IEEE Int. Conf. on Robotics and Biomimetics (ROBIO) (Kuala Lumpur, Malaysia) pp 1287–91
[20] Sullivan A, Xia H, McBride J and Zhao X 2010 Reconstruction of missing physiological signals using artificial neural networks 2010 Computing in Cardiology (Belfast) pp 317–20
[21] Duda J 2018 Exploiting statistical dependencies of time series with hierarchical correlation reconstruction (arXiv:1807.04119)
[22] Tian W, Liu Z, Li L, Zhang S and Li C 2020 Identification of abnormal conditions in high-dimensional chemical process based on feature selection and deep learning Chin. J. Chem. Eng. 28 1875–83
[23] Duda J 2018 Hierarchical correlation reconstruction with missing data, for example for biology-inspired neuron (arXiv:Learning)
[24] Crosse M J, Butler J S and Lalor E C 2015 Congruent visual speech enhances cortical entrainment to continuous auditory speech in noise-free conditions J. Neurosci. 35 14195–204
[25] Seimon A 2003 Improving climatic signal representation in tropical ice cores: a case study from the Quelccaya Ice Cap, Peru Geophys. Res. Lett. 30 772–1
[26] Robertson I, Loader N J, McCarroll D, Carter A H C, Cheng L and Leavitt S W 2004 δ13C of tree-ring lignin as an indirect measure of climate change Water Air Soil Pollut. Focus 4 531–44
[27] Allen K, Drew D M, Downes G M, Evans R, Baker P and Grose M 2012 Ring width, climate and wood density relationships in two long-lived Tasmanian tree species Dendrochronologia 30 167–77
[28] Pan Z, Hu Y and Cao B 2017 Construction of smooth daily remote sensing time series data: a higher spatiotemporal resolution perspective Open Geospatial Data Softw. Stand. 2 1–11
[29] Sidekerskiene T and Damaševiˇcius R 2016 Reconstruction of missing data in synthetic time series using EMD
[30] Oriani F, Borghi A, Straubhaar J, Mariethoz G and Renard P 2016 Missing data simulation inside flow rate time-series
using multiple-point statistics Environ. Model. Softw. 86 264–76 ISSN 1364-8152
[31] Kalalas C and Alonso-Zarate J 2020 Sensor data reconstruction in industrial environments with cellular connectivity 2020 IEEE 31st Annual Int. Symp. on Personal, Indoor and Mobile Radio Communications (London, United Kingdom) pp 1–6
[32] Hippert-Ferrer A, Yan Y, Bolon P and Millan R 2020 Spatiotemporal filling of missing data in remotely sensed displacement measurement time series IEEE Geosci. Remote Sens. Lett. 1–5
[33] Hippert-Ferrer A, Yan Y and Bolon P 2019 Gap-filling based on iterative EOF analysis of temporal covariance: application to InSAR displacement time series IGARSS 2019-2019 IEEE Int. Geoscience and Remote Sensing Symp. (Yokohama, Japan) pp 262–5
[34] Bertoluzza M, Paris C and Bruzzone L 2019 A fast method for cloud removal and image restoration on time series of multispectral images 2019 10th Int. Workshop on the Analysis of Multitemporal Remote Sensing Images (Multitemp) (Shanghai, China) pp 1–4
[35] Chen L, Wang L, Zhao J and Wang W 2021 Relevance vector machines-based time series prediction for incomplete training dataset: two comparative approaches IEEE Trans. Cybern. 51 4298–311
[36] Wang Y, Zhang Y, Piao X, Liu H and Zhang K 2019 Traffic data reconstruction via adaptive spatial-temporal correlations IEEE Trans. Intell. Trans. Syst. 20 1531–43
[37] Miao T 2018 Research of regional drought forecasting based on phase space reconstruction and wavelet neural network model 2018 7th Int. Conf. on Agro-geoinformatics (Agro-geoinformatics) (Hangzhou) pp 1–4
[38] Quevedo J, Pesantez J L, Espin S, Roquet J and Valero F 2018 Animprovedtoolofwaterdataanalyticsforflowmetersdata: application to the Barcelona supra-municipal distribution water network 2018 Int. Workshop on Cyber-physical Systems for Smart Water Networks (Cyswater) (Porto) pp 1–4
[39] Valero S, Pelletier C and Bertolino M 2016 Patch-based reconstruction of high resolution satellite image time series with missing values using spatial, spectral and temporal similarities 2016 IEEE Int. Geoscience and Remote Sensing Symp. (IGARSS) (Beijing) pp 2308–11
[40] Yu F and Zhijie S 2015 Methods of real-time data screening and reconstruction for dynamic traffic abnormal data 2015 6th Int. Conf. on Intelligent Systems Design and Engineering Applications (ISDEA) (Guiyang) pp 500–3
[41] Liu L, Zhang J, Li P, Zhang Y and Hu X 2016 A label correlation based weighting feature selection approach for multi-label data Web-Age Information Management. WAIM 2016 (Lecture Notes in Computer Science vol 9659) vol 9659 ed B Cui, N Zhang, J Xu, X Lian and D Liu (Berlin: Springer) (https://doi.org/10.1007/978-3-319-39958-4_29)
[42] Zhang H and Sheng S 2004 Learning weighted naive Bayes with accurate ranking Proc. 4th Int. Conf. Data Mining pp 567–70
[43] Jiang L, Zhang L, Li C and Wu J 2019 A correlation-based feature weighting filter for naive Bayes IEEE Trans. Knowl. Data Eng. 31 201–13
[44] El Harchi M 2016 Finding redundant data sources in smart environments Master Thesis Eindhoven University of Technology (February)
[45] Ramakrishnan A G and Satyanarayana J V 2016 Reconstruction of EEG from limited channel acquisition using estimated signal correlation Biomed. Signal Process. Control. 27 164–73